Electrical Power and Energy Systems 41 (2012) 34–43

Contents lists available at SciVerse ScienceDirect

Electrical Power and Energy Systems

journal homepage: www.elsevier.com/locate/ijepes

Load compensation using DSTATCOM in three-phase, three-wire distribution system under various source voltage and delta connected load conditions

Tejas Zaveri [a,*], B.R. Bhalja [b], Naimish Zaveri [c]

[a] Faculty of Engineering & Technology, Veer Narmad South Gujarat University, Surat 395 007, Gujarat, India
[b] Department of Electrical Engineering, A.D. Patel Institute of Technology, New Vallabh Vidyanagar 388 121, Gujarat, India
[c] Electrical Engineering Department, C.K. Pithawalla College of Engineering & Technology, Surat 395 007, Gujarat, India

ARTICLE INFO

Article history:
Received 25 October 2011
Received in revised form 19 December 2011
Accepted 5 February 2012
Available online 15 March 2012

Keywords:
DSTATCOM
IARCC theory
Power factor correction
Source VA reduction
Load balancing
Harmonic mitigation

ABSTRACT

This paper deals with a Distribution STATic COMpensator (DSTATCOM) for balancing of source currents, power factor correction and harmonic mitigation in three-phase, three-wire distribution system supplying delta connected load under various source voltage conditions. The control strategy applied to the DSTATCOM play a major role in its performance. A novel approach based on an improved instantaneous active and reactive current component (IARCC) theory is proposed for generation of three-phase reference currents for DSTATCOM. A three-phase voltage source converter with a dc bus capacitor is employed as DSTACOM which will track the reference currents in a hysteresis band scheme. The performance of DSTATCOM is evaluated under sinusoidal, unbalanced sinusoidal and unbalanced distorted source voltage conditions. Variation in load current, variation in magnitude and harmonic content in source voltage has been considered. Delta connected linear as well as non-linear load conditions have been considered. The performance of the DSTATCOM using the proposed control strategy is demonstrated using simulation results in MATLAB/SIMULINK software. Simulation results demonstrate the feasibility of proposed scheme for the control of DSTACOM.

1. Introduction

Nowadays, the power quality in the distribution system is contaminated due to high reactive power burden, distorted and unbalance load currents [1–3]. Due to excessive reactive power demand, there is an increase in transmission & distribution losses and reduction in active power flow capability of the distribution system. Further, the operation of transformers and generators are also affected due to unbalancing of currents and it also increases the size of utility [4]. Therefore, reactive power compensation of non-linear and/or poor power factor loads and load balancing is an important issue in the modern power distribution system. The power indices are governed by various standards such as IEEE-519 standard [5]. The remedies to power quality problems are reported in literature and are known by the generic name of custom power devices [3].

Dynamic voltage restorer (DVR) is a custom power device connected in series with the load. The basic principle of a DVR is based on restoration of the load side voltage to the desired amplitude and waveform irrespective of unbalance or distortion in either source or load side by inserting a voltage of required magnitude and frequency. Thus, it protects sensitive load from the effect of unbalance and/or distortion in the supply side voltage [6]. Therefore, DVR is not suitable to serve objectives such as harmonic mitigation in source currents due to non-linear load, imbalance elimination of unbalanced loads, supply power factor correction and source VA reduction under various source voltage and load conditions. Conversely, DSTATCOM is a custom power device connected in shunt with the load. It injects currents in the ac system such that the load compensation is achieved irrespective of unbalance or distortion in either source or load side. Moreover, it is operated in current control mode to compensate the effect of load currents under various source voltage conditions. Further, it is very effective in balancing of any unbalance in load currents and also for cleaning pollution in the load. In this way, it protects the utility system from the ill effects of customer loads [6].

DSTATCOM has been used extensively for reactive power compensation, balancing of source currents and harmonic compensation in the distribution system [7]. The performance of DSTATCOM depends on the reference current generation technique. To serve this purpose, many control algorithms have been presented by various researchers. These algorithms are based on instantaneous reactive power theory, synchronous reference frame theory (SRF), symmetrical component theory, current compensation technique using dc bus voltage regulation, computation tech-

* Corresponding author. Tel.: +91 9909110232.
E-mail addresses: zaveritejas@yahoo.com (T. Zaveri), bhaveshbhalja@gmail.com (B.R. Bhalja), zaverinaimish@yahoo.com (N. Zaveri).

0142-0615/$ - see front matter © 2012 Elsevier Ltd. All rights reserved.
doi:10.1016/j.ijepes.2012.02.015

Nomenclature

$V_{sa/b/c}$	source voltage of phase-a, phase-b and phase-c respectively
$i_{sa/b/c}$	source current of phase-a, phase-b and phase-c respectively
$i_{lab/bc/ca}$	load currents
$i_{stab/bc/ca}$	compensator currents
~	over the letter: variable part
–	over the letter: average value

Subscript

d	d component in odq coordinates system
q	q component in odq coordinates system
α	α component in $0\alpha\beta$ coordinates system
αF	α component in $0\alpha\beta$ coordinates system after filtration
β	β component in $0\alpha\beta$ coordinates system
βF	β component in $0\alpha\beta$ coordinates system after filtration
$1h$	fundamental component
nh	nth harmonic component

Superscript

+	positive sequence component
–	negative sequence component
*	reference component

nique based on per phase basis and schemes based on neural network techniques, adaline-based control algorithm [2,8–17].

In order to mitigate harmonics, the instantaneous active and reactive current component (i_d–i_q) method had been proposed by researcher for shunt active filter [18]. It has been observed from literature survey that most of the earlier work for power quality improvement using DSTATCOM was on 3-phase, 3-wire system under sinusoidal source voltage condition. However, not much attention has been paid to 3-phase, 3-wire power distribution system, particularly for unbalanced and non sinusoidal source voltage conditions with delta connected load.

The balancing of an unbalanced delta connected load is a classical problem. An excellent description of load balancing is given in [19] in which any unbalanced reactive delta-connected network is converted into a balanced resistive delta-connected network by suitable introduction of admittance in parallel with each branch. The solution, even though aesthetically pleasing has been carried out only for sinusoidal steady state conditions.

In this paper, a DSTATCOM controlled by novel control strategy to serve the following objectives:

- To cancel the effect of unbalanced loads such that current drawn from the source are balanced.
- To eliminate the effect of poor load power factor such that source has almost unity power factor.
- To compensate the effect of non-linear loads due to its harmonic content such that currents drawn from the source are sinusoidal under any source voltage condition.
- To reduce source VA for given source voltage and load conditions.

2. Improved instantaneous active and reactive current component method

Fig. 1 shows the basic block diagram of the proposed method. The transformation angle is obtained with the voltages of the ac network. The major difference between the proposed method and SRF method [9] is that the speed of the reference frame is no longer constant due to voltage harmonics and imbalance. It varies instantaneously depending on the waveform of the three phase voltages of the system.

In the proposed scheme, the compensating currents are obtained from the instantaneous active and reactive current components of the load. Load currents in stationary ($\alpha\beta$) reference frame are obtained by applying Clarke's transformation as given by following equation.

$$\begin{bmatrix} i_{l\alpha} \\ i_{l\beta} \end{bmatrix} = \sqrt{\frac{2}{3}} \begin{bmatrix} 1 & -1/2 & -1/2 \\ 0 & \sqrt{3}/2 & -\sqrt{3}/2 \end{bmatrix} \begin{bmatrix} i_{lab} \\ i_{lbc} \\ i_{lca} \end{bmatrix} \tag{1}$$

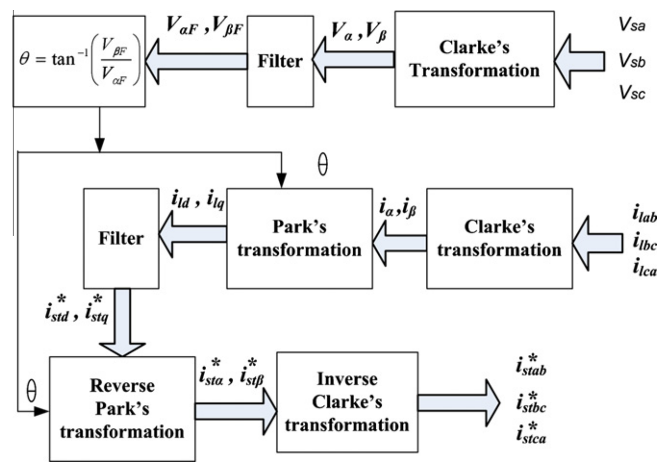

Fig. 1. Basic block diagram of proposed scheme.

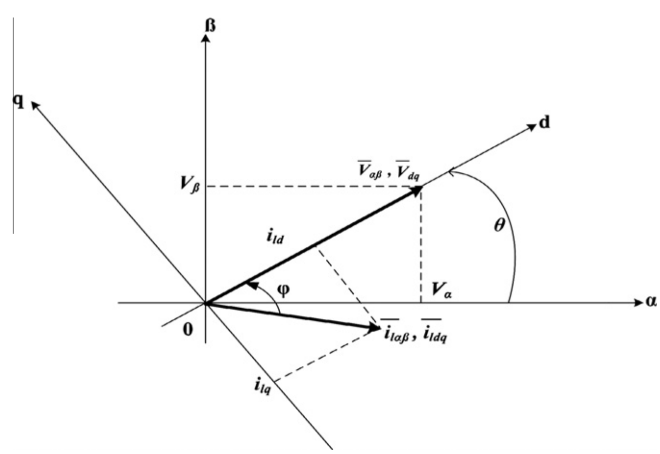

Fig. 2. Voltage and current space vectors in the stationary and synchronous reference frames.

Source voltages in stationary ($\alpha\beta$) reference frame are obtained by applying Clarke's transformation as given by following equation.

$$\begin{bmatrix} V_\alpha \\ V_\beta \end{bmatrix} = \sqrt{\frac{2}{3}} \begin{bmatrix} 1 & -1/2 & -1/2 \\ 0 & \sqrt{3}/2 & -\sqrt{3}/2 \end{bmatrix} \begin{bmatrix} V_{sa} \\ V_{sb} \\ V_{sc} \end{bmatrix} \tag{2}$$

In order to calculate the transformation angle, source voltages in stationary ($\alpha\beta$) reference frame given by Eq. (2) are filtered by low pass filters. Source voltages in stationary reference frame after filtering are denoted by $V_{\alpha F}$ and $V_{\beta F}$. The use of the low pass filter makes the strategy more insensitive to harmonics on the mains.

The magnitude response of Butterworth low-pass filter is given by,

$$|H(j\omega)| = \frac{A}{\left[1 + (\Omega/\Omega_C)^{2N}\right]^{0.5}}$$

where A is the filter gain and Ω_C is the 3 dB cut-off frequency and N is the order of the filter.

The transfer function of the Butterworth filter is usually written in the factored form as given below

$$H(S) = \prod_{K=1}^{N/2} \frac{B_k \Omega_C^2}{s^2 + b_k \Omega_C s + c_k \Omega_C^2} \quad N = 2, 4, 6, \ldots$$

or

$$H(S) = \frac{B_0 \Omega_C}{s + c_0 \Omega_C} \prod_{K=1}^{(N-1)/2} \frac{B_k \Omega_C^2}{s^2 + b_k \Omega_C s + c_k \Omega_C^2} \quad N = 3, 5, 7, \ldots$$

The coefficients b_k and c_k are given by,

$$b_k = 2\sin[(2k-1)\pi/2N] \quad \text{and } C_k = 1$$

The parameters B_k can be obtained from the following equations.

$$A = \prod_{K=1}^{N/2} B_K, \text{for even } N$$

and

$$A = \prod_{K=1}^{(N-1)/2} B_K, \text{for odd } N$$

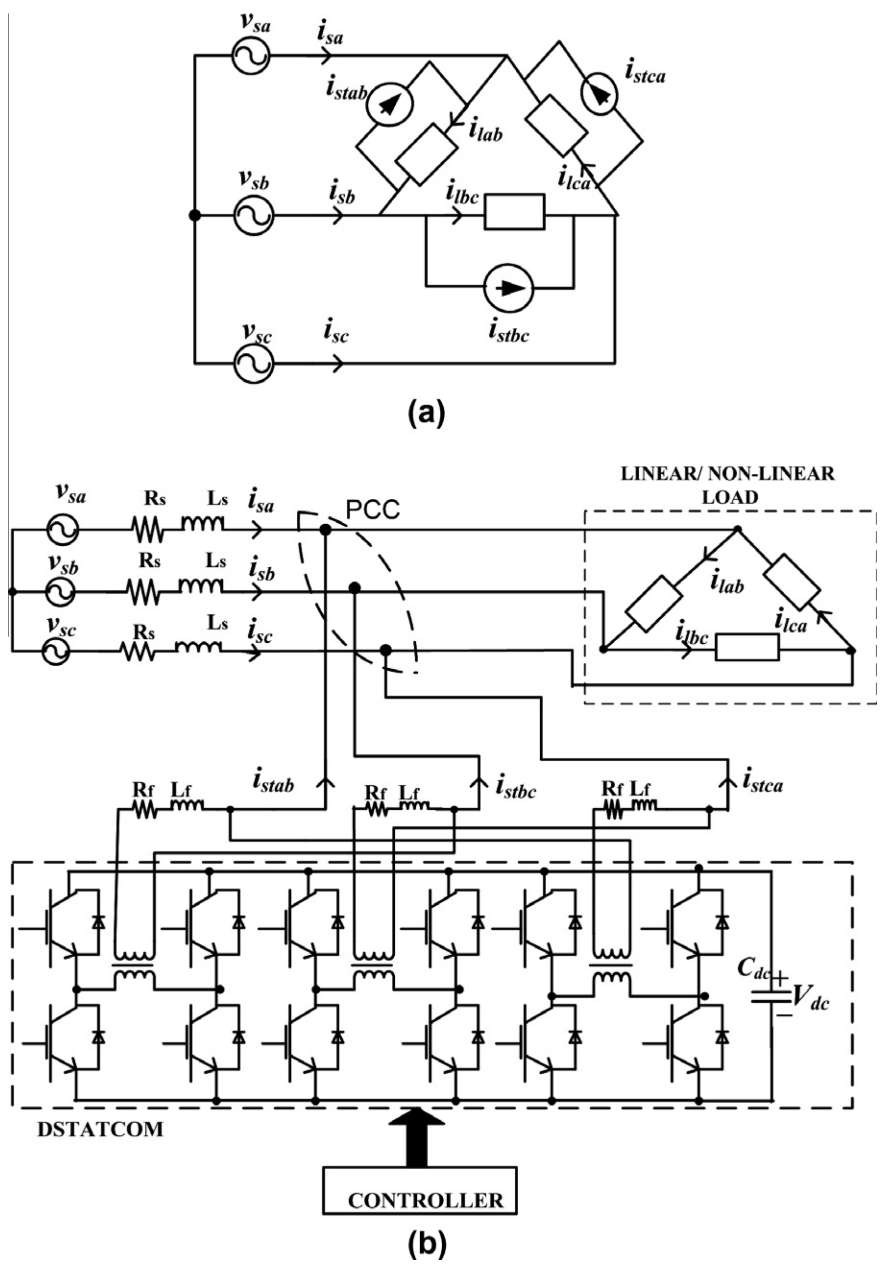

Fig. 3. (a) Basic compensator scheme and (b) system configuration with practical realization of compensator.

Load currents in rotating (dq) reference frame are obtained by applying Park's transformation as shown in following equation.

$$\begin{bmatrix} i_{ld} \\ i_{lq} \end{bmatrix} = \begin{bmatrix} \cos\theta & \sin\theta \\ -\sin\theta & \cos\theta \end{bmatrix} \begin{bmatrix} i_{l\alpha} \\ i_{l\beta} \end{bmatrix}, \theta = \tan^{-1}\left(\frac{V_{\beta F}}{V_{\alpha F}}\right) \tag{3}$$

Fig. 2 depicts the voltage and current space vectors in the stationary ($\alpha\beta$) and rotating reference frames (dq). Under balanced and sinusoidal mains voltage conditions, the transformation angle θ is a function of time and it increases uniformly. Therefore, $d\theta/dt$ does not remain constant over a period of supply voltage. Now, due to transformation, the direct and the quadrature components of voltage are given by,

$$V_d = |\overline{V}_{dq}| = |\overline{V}_{\alpha\beta}| = \sqrt{V_{\alpha F}^2 + V_{\beta F}^2} \quad \text{and } V_q = 0.$$

If d-axis is in the direction of the voltage space vector then the transformation is given by Eq. (4). This is achieved by substituting $\cos\theta = \frac{V_{\alpha F}}{\sqrt{V_{\alpha F}^2 + V_{\beta F}^2}}$ and $\sin\theta = \frac{V_{\beta F}}{\sqrt{V_{\alpha F}^2 + V_{\beta F}^2}}$ into following equation.

$$\begin{bmatrix} i_{ld} \\ i_{lq} \end{bmatrix} = \frac{1}{\sqrt{V_{\alpha F}^2 + V_{\beta F}^2}} \begin{bmatrix} V_{\alpha F} & V_{\beta F} \\ -V_{\beta F} & V_{\alpha F} \end{bmatrix} \begin{bmatrix} i_{l\alpha} \\ i_{l\beta} \end{bmatrix} \tag{4}$$

Instantaneous active and reactive load currents in rotating reference frame, i_{ld} and i_{lq} can be decomposed into oscillatory and average terms as under.

$$i_{ld} = \bar{i}_{ld} + \tilde{i}_{ld} \quad \text{and } i_{lq} = \bar{i}_{lq} + \tilde{i}_{lq}.$$

The positive sequence component of first harmonic current is transformed into dc quantities (i^{+}_{ldq1h}) which constitutes the average current components. All higher order current harmonics including the negative sequence component of first harmonic current ($i^{\pm}_{ldqnh} + i^{-}_{ldq1h}$) are transformed into non-dc quantities and undergo a frequency shift in the spectra. Hence, they constitute the oscillatory current components. The fundamental currents of d–q components are now dc values and harmonics are going to appear like a ripple. Harmonic isolation of d–q transformed signal is achieved by removing the dc offset. After eliminating the average current components by filters, the reference compensator currents are obtained as under.

$$i^*_{std} = -\tilde{i}_{ld} \quad \text{and } i^*_{std} = -\tilde{i}_{lq}$$

Therefore, the reference currents of voltage source converter in the $\alpha\beta$ coordinates are obtained by applying Inverse Park transformation and given by following equation.

$$\begin{bmatrix} i^*_{st\alpha} \\ i^*_{st\beta} \end{bmatrix} = \frac{1}{\sqrt{V_{\alpha F}^2 + V_{\beta F}^2}} \begin{bmatrix} V_{\alpha F} & -V_{\beta F} \\ V_{\beta F} & V_{\alpha F} \end{bmatrix} \begin{bmatrix} i^*_{std} \\ i^*_{stq} \end{bmatrix} \tag{5}$$

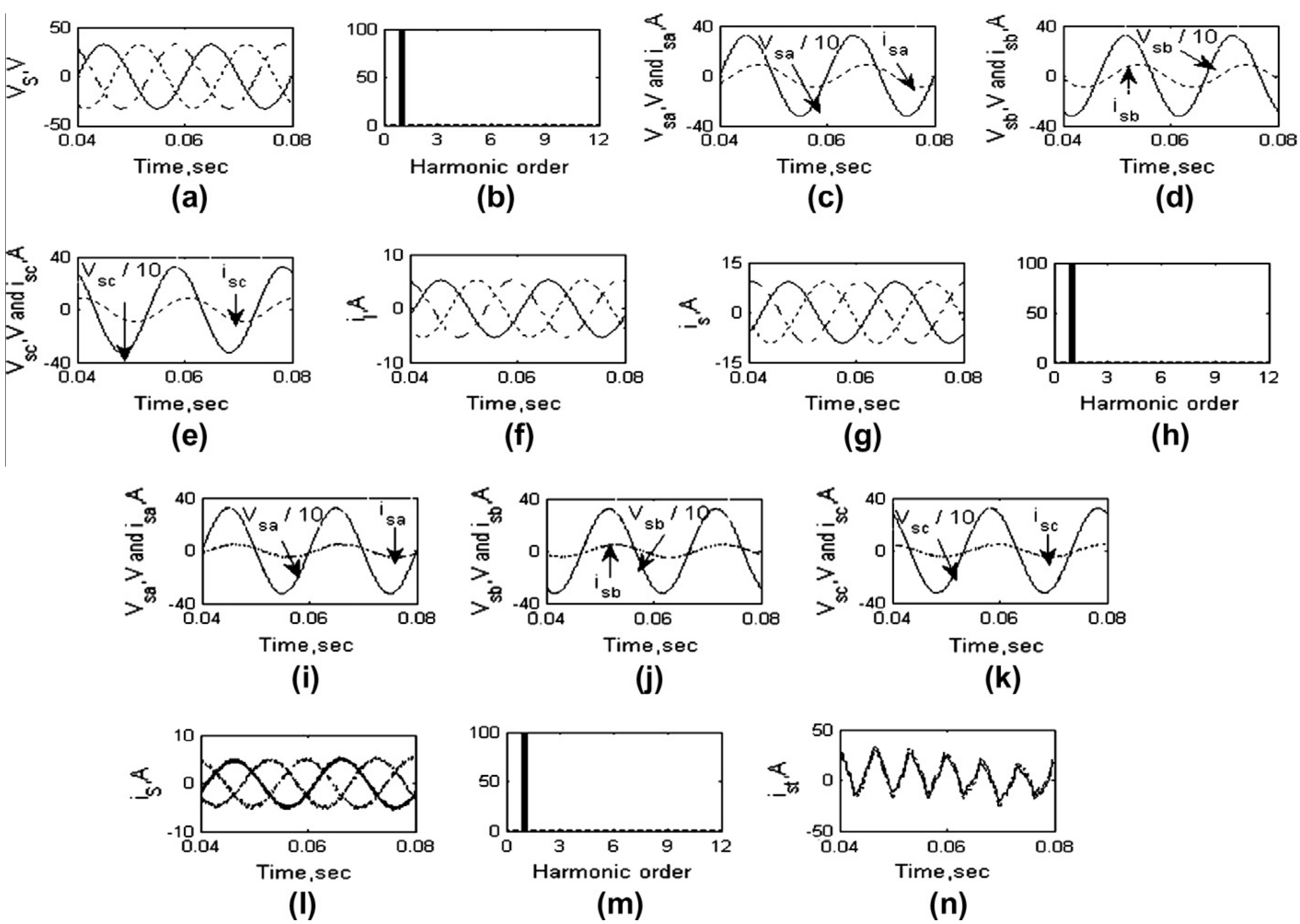

Fig. 4. DSTATCOM performance for linear balanced load under case A: (a) three-phase source voltages, (b) FFT spectrum of source voltage of phase-a, (c) source voltage and uncompensated source current of phase-a, (d) source voltage and uncompensated source current of phase-b, (e) source voltage and uncompensated source current of phase-c, (f) three-phase load currents, (g) three-phase uncompensated source currents, (h) FFT spectrum of uncompensated source current of phase-a, (i) source voltage and compensated source current of phase-a, (j) source voltage and compensated source current of phase-b, (k) source voltage and compensated source current of phase-c, (l) three-phase source currents after compensation, (m) FFT spectrum of compensated source current of phase-a, (n) three-phase compensator currents.

Applying Inverse Clarke's transformation, the reference currents of voltage source converter in abc frame are given by following equation.

$$\begin{bmatrix} i^*_{stab} \\ i^*_{stbc} \\ i^*_{stca} \end{bmatrix} = \sqrt{\frac{2}{3}} \begin{bmatrix} 1 & -1/2 & -1/2 \\ 0 & \sqrt{3}/2 & -\sqrt{3}/2 \end{bmatrix}^T \begin{bmatrix} i^*_{st\alpha} \\ i^*_{st\beta} \end{bmatrix} \tag{6}$$

3. System configuration

The basic compensator scheme for delta connected load is shown in Fig. 3a. Fig. 3b shows the system configuration with the practical realization of the compensator for the proposed scheme. The compensator can be implemented by a three-phase voltage source converter (VSC) which has been operated in hysteresis band control scheme to track reference currents generated by the proposed control algorithm.

The structure of the compensator contains a bank of three single-phase VSC units. Three single-phase voltage source converters are connected to a common dc storage capacitor. Each VSC unit is connected through an isolating transformer which provides isolation between the converters. In Fig. 3b, controlled switch is a power semiconductor device and anti-parallel diode combination. Transformer also prevents the dc storage capacitor from being shorted through controlled switches in different converters. It is to be noted that the capacitor must be pre-charged to sufficiently high value in order to obtain satisfactory tracking performance. However, increasing the capacitor voltage increases the losses in the system. Therefore, the level of capacitor voltage must be chosen judiciously. L_f represents the inductance of each transformer as well as an additional interfacing inductance. It has been used to filter out high-frequency components of compensating currents. It also controls the switching frequency of the inverter which is limited by the speed of switching devices and the power level.

4. Performance evaluation

The proposed control algorithm is validated using MATLAB/SIMPOWER software. In this section, simulation results of three-phase, three-wire system supplying delta connected linear/non-linear load under various source voltage conditions are presented. Linear load is realized by resistive-inductive load whereas non-linear load is simulated by three-phase rectifier with RLC load. The system parameters are given in Appendix A.

Simulation study has been carried out with linear/non-linear load under three different source voltage conditions:

Case A: ideal source voltage.
Case B: unbalanced sinusoidal source voltage.
Case C: unbalanced distorted source voltage.

In order to plot source voltages and currents on the same scale, source voltages are scaled down by a factor of 10 and 2 for linear and non-linear load, respectively.

4.1. Ideal source voltage (Case A)

For balanced sinusoidal source voltage condition, performance of DSTATCOM with linear and non-linear load is shown in Figs. 4

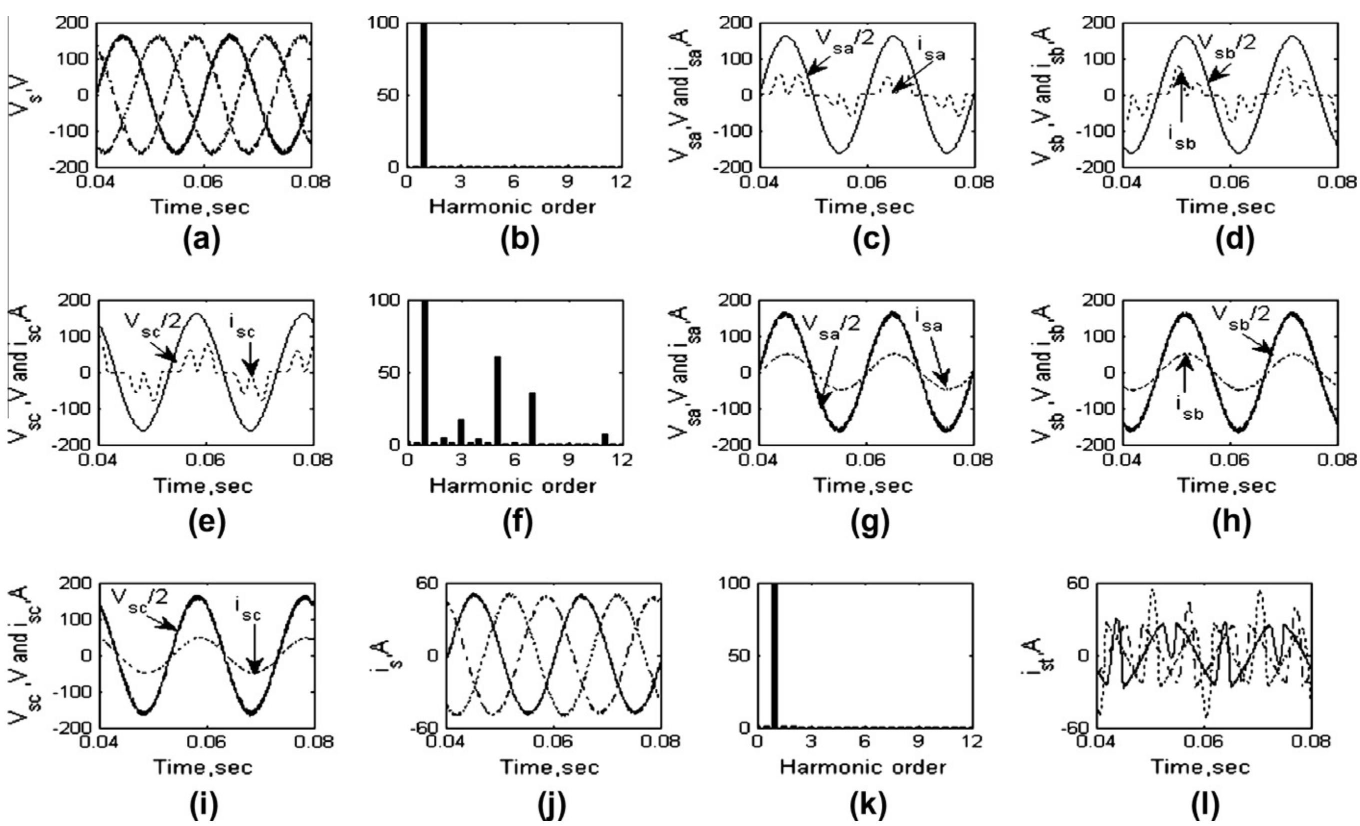

Fig. 5. DSTATCOM performance for non-linear unbalanced load under case A: (a) three-phase source voltages, (b) FFT spectrum of source voltage of phase-a, (c) source voltage and uncompensated source current of phase-a, (d) source voltage and uncompensated source current of phase-b, (e) source voltage and uncompensated source current of phase-c, (f) FFT spectrum of uncompensated source current of phase-a, (g) source voltage and compensated source current of phase-a, (h) source voltage and compensated source current of phase-b, (i) source voltage and compensated source current of phase-c, (j) three-phase source currents after compensation, (k) FFT spectrum of compensated source current of phase-a, (l) three-phase compensator currents.

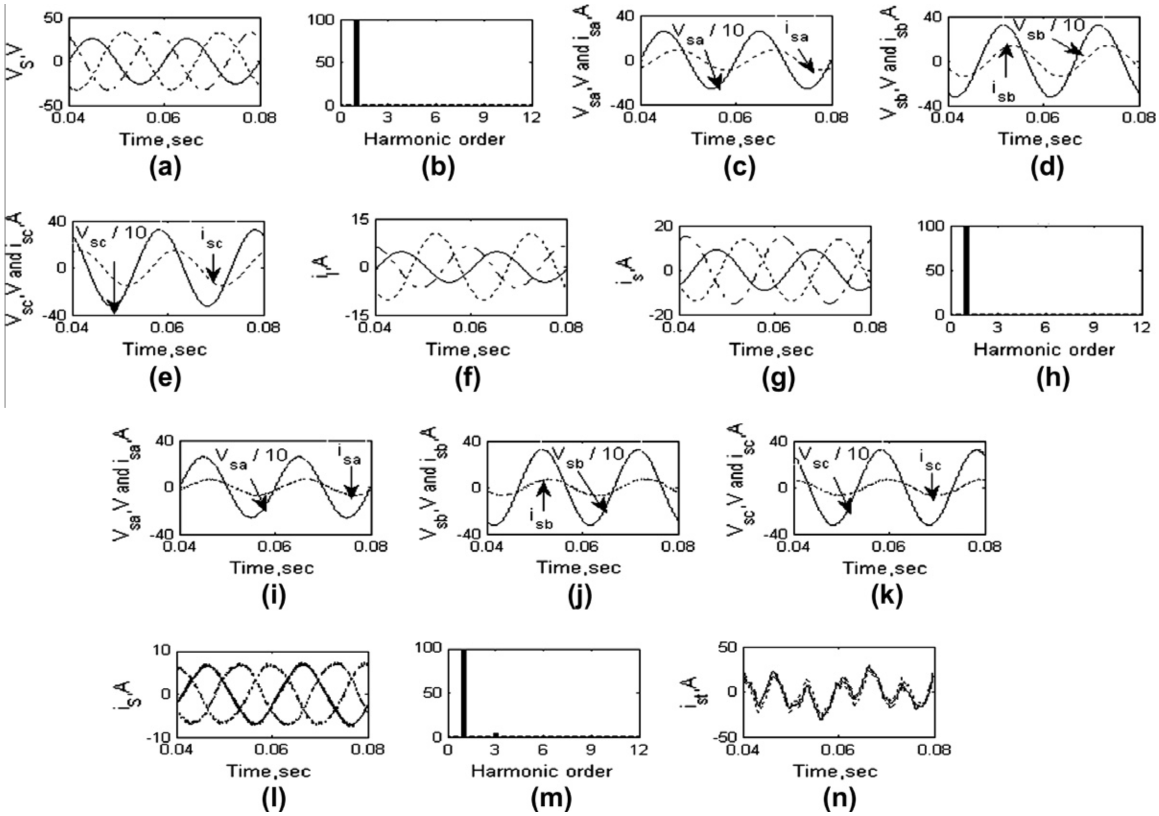

Fig. 6. DSTATCOM performance for linear unbalanced load under case B:(a) three-phase source voltages, (b) FFT spectrum of source voltage of phase-a, (c) source voltage and uncompensated source current of phase-a, (d) source voltage and uncompensated source current of phase-b, (e) source voltage and uncompensated source current of phase-c, (f) three-phase load currents, (g) three-phase uncompensated source currents, (h) FFT spectrum of source current of phase-a, (i) source voltage and compensated source current of phase-a, (j) source voltage and compensated source current of phase-b, (k) source voltage and compensated source current of phase-c, (l) three-phase source currents after compensation, (m) FFT spectrum of compensated source current of phase-a, (n) three-phase compensator currents.

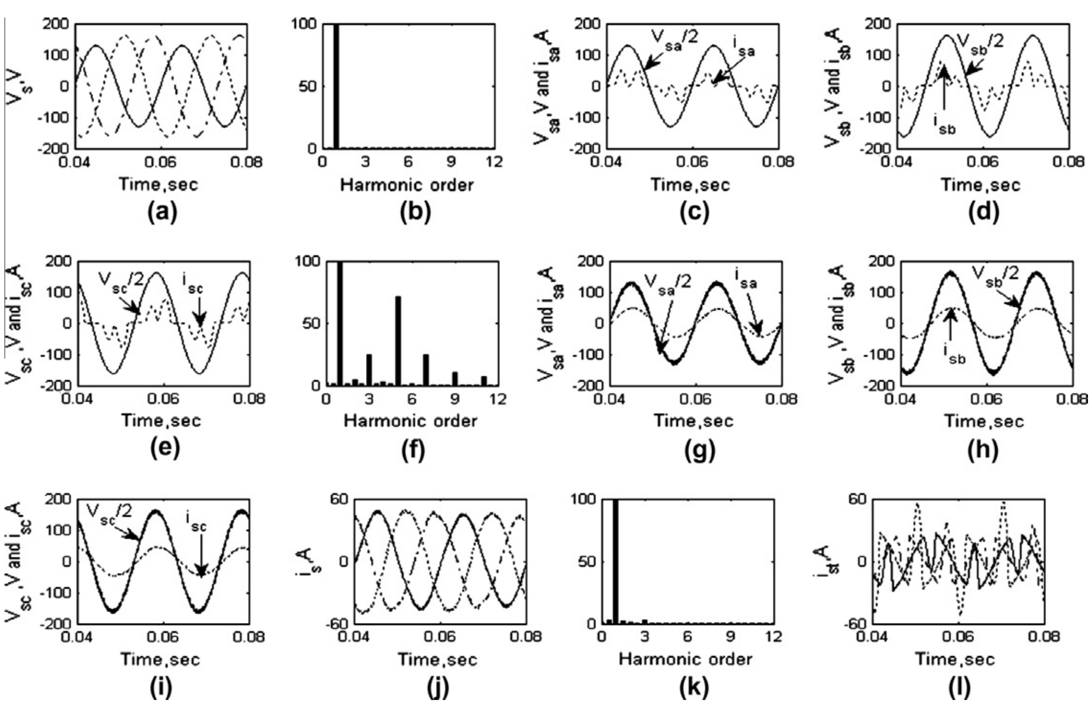

Fig. 7. DSTATCOM performance for non-linear unbalanced load under case B:(a) three-phase source voltages, (b) FFT spectrum of source voltage of phase-a, (c) source voltage and uncompensated source current of phase-a, (d) source voltage and uncompensated source current of phase-b, (e) source voltage and uncompensated source current of phase-c, (f) FFT spectrum of uncompensated source current of phase-a, (g) source voltage and compensated source current of phase-a, (h) source voltage and compensated source current of phase-b, (i) source voltage and compensated source current of phase-c, (j) three-phase source currents after compensation, (k) FFT spectrum of compensated source current of phase-a, (l) three-phase compensator currents.

and 5, respectively. For linear load, balanced load currents have been considered. It has been observed from Fig. 4 that under uncompensated condition, source voltage is not in alignment with source current. It indicates that reactive power is supplied by source. Correction in supply power factor can be observed after compensation. We can observe reduction in magnitude of source currents compared to uncompensated source currents. With reference to Fig. 5, it is to be noted that source currents have become almost sinusoidal for highly distorted load currents. Compensated source current consist of only fundamental component where as no. of harmonics are present in uncompensated source currents. Moreover, balancing of source currents and unity power factor are obtained. Only average component of load power is supplied by source.

4.2. Unbalanced sinusoidal source voltage (Case B)

The magnitude of source voltage of phase-a is 20% smaller than source voltage of phase-b and phase-c. Simulation results of case B with linear and non-linear unbalanced load are shown in Figs. 6 and 7, respectively. It is to be noted from Figs. 6 and 7 that irrespective of unbalancing in source voltages, it is possible to achieve power factor correction, reduction in magnitude of source currents and balancing of source currents. Effect of unbalance in source voltages is observed in compensator currents compared to case A. In case of non-linear load, it can be observed from FFT spectrum that odd order harmonics are present in uncompensated source currents whereas only fundamental component is present in compensated source current. Thus, harmonic mitigation is achieved effectively which results in sinusoidal source currents.

4.3. Unbalanced distorted source voltage (Case C)

For this case, source voltages are unbalanced and distorted. The magnitude of source voltage of phase-a is 20% smaller than the rated source voltage. Fifth harmonic with amplitude 1/10 and seventh harmonic component with amplitude of 1/14 of the rated source voltage are present in source voltage of phase-a and phase-b, respectively. Moreover, Fifth harmonic and seventh harmonic with their amplitudes same as in phase-a and phase-b, respectively are simultaneously present in source voltage of phase-c. Figs. 8 and 9 show the simulation results of DSTATCOM for linear and non-linear unbalanced load, respectively. For non-linear unbalance load, both source voltages and load currents are distorted and unbalanced. Hence, the condition has become more critical. It has been observed from Figs. 8 and 9 that source currents become almost equal in magnitude. It can be noted from FFT spectrum of compensated source current that only fundamental component is present in source current after compensation. Thus, irrespective of variation in harmonic content in each phase of source voltage, harmonic mitigation is effectively achieved. Further, due to reduction in magnitude of compensated source

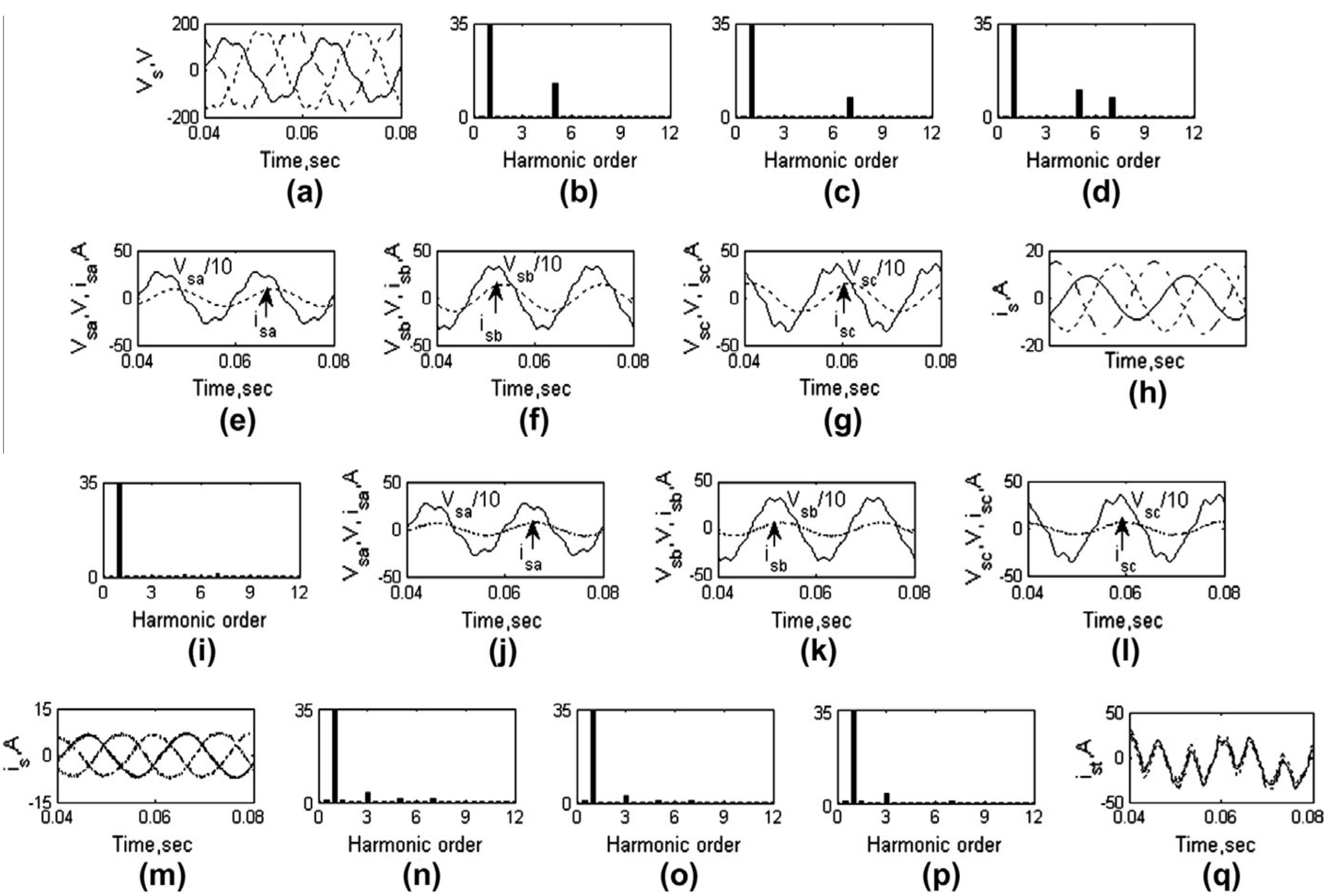

Fig. 8. DSTATCOM performance for linear unbalanced load under case C:(a) three-phase source voltages, (b) FFT spectrum of source voltage of phase-a, (c) FFT spectrum of source voltage of phase-b, (d) FFT spectrum of source voltage of phase-c, (e) source voltage and uncompensated source current of phase-a, (f) source voltage and uncompensated source current of phase-b, (g) source voltage and uncompensated source current of phase-c, (h) three-phase uncompensated source currents, (i) FFT spectrum of uncompensated source current of phase-a, (j) source voltage and compensated source current of phase-a, (k) source voltage and compensated source current of phase-b, (l) source voltage and compensated source current of phase-c, (m) three-phase source currents after compensation, (n) FFT spectrum of compensated source current of phase-a, (o) FFT spectrum of compensated source current of phase-b, (p) FFT spectrum of compensated source current of phase-c, (q) three-phase compensator currents.

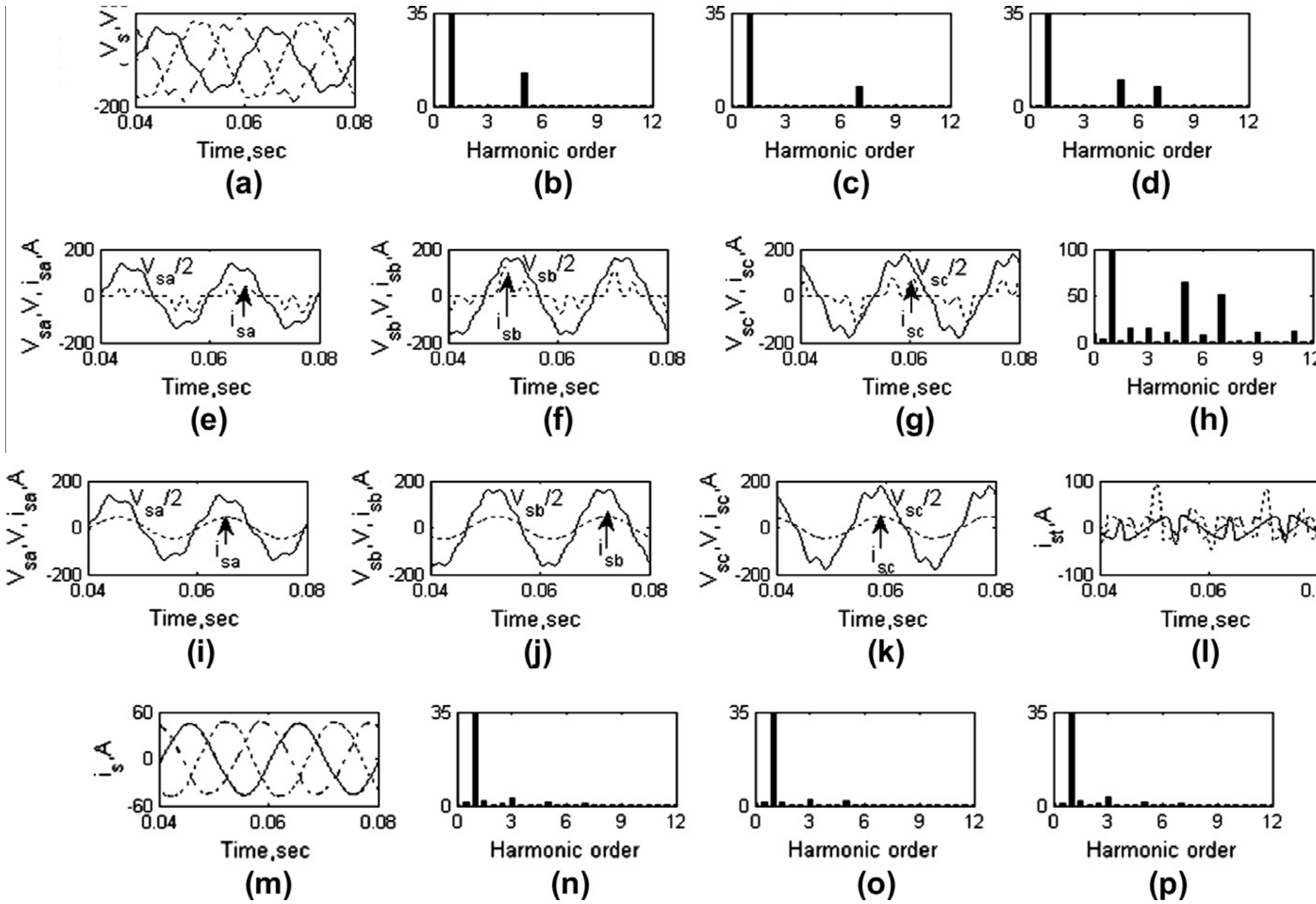

Fig. 9. DSTATCOM performance for non-linear unbalanced load under case C:(a) three-phase source voltages, (b) FFT spectrum of source voltage of phase-a, (c) FFT spectrum of source voltage of phase-b, (d) FFT spectrum of source voltage of phase-c, (e) source voltage and uncompensated source current of phase-a, (f) source voltage and uncompensated source current of phase-b, (g) source voltage and uncompensated source current of phase-c, (h) FFT spectrum of uncompensated source current of phase-a (i) source voltage and compensated source current of phase-a, (j) source voltage and compensated source current of phase-b, (k) source voltage and compensated source current of phase-c, (l) three-phase compensator currents, (m) three-phase source currents after compensation, (n) FFT spectrum of compensated source current of phase-a, (o) FFT spectrum of compensated source current of phase-b, (p) FFT spectrum of compensated source current of phase-c.

current, source VA is reduced. Power factor improvement is obtained with linear as well as non-linear load.

4.4. Results and discussion

Source voltage data along with total harmonic distortion (THD), load currents, uncompensated source current data for linear load under three different cases, as discussed in the previous sub-sections are shown in Table 1. It is to be noted from Table 1 that the percentage THD for unbalanced distorted source voltage (case C) is above 7% which is higher than IEEE-519 standard harmonic voltage limits [5].

Supply voltage data for non-linear load are same as that for linear load mentioned in Table 1. Table 2 show load current, uncompensated source current data along with THD for non-linear load under above mentioned three cases.

It has been observed from simulation results that the uncompensated source current and the source voltage of the respective phase are not in alignment for linear as well as non-linear load under various source voltage conditions. Therefore, source has to supply reactive power if compensator is not available. Further, uncompensated source currents are unbalanced. In addition, source currents without compensation are highly distorted in case of non-linear unbalanced load and hence, the percentage THD exceeds (very high) above IEEE-519 standard harmonic current limits.

Tables 3 and 4 show the simulation results of the proposed control strategy under three different cases with linear as well as non-linear load, respectively.

Table 1
Source voltage, load current, uncompensated source current data for linear load.

Case	Source voltages						Load currents			Source currents		
	V_{sa}		V_{sb}		V_{sc}		i_{lab}	i_{lbc}	i_{lca}	i_{sa}	i_{sb}	i_{sc}
	rms (V)	THD (%)	rms (V)	THD (%)	rms (V)	THD (%)	rms (A)	rms (A)	rms (A)	rms (A)	rms (A)	rms (A)
A	229.7	0	229.7	0	229.7	0	3.74	3.74	3.74	6.47	6.47	6.47
B	183.6	0	229.2	0	229.4	0	3.37	7.38	4.60	6.48	9.82	10.68
C	185.4	12.5	230.6	7.20	231.7	12.32	3.38	7.41	4.61	6.45	9.85	10.71

Table 2
Load current, uncompensated source current data for non-linear load.

Case	Load currents								Source currents			
	i_{lab}		i_{lbc}		i_{lca}		i_{sa}		i_{sb}		i_{sc}	
	rms (A)	THD (%)	rms (A)	THD (%)	rms (A)	THD (%)	rms (A)	THD (%)	rms (A)	THD (%)	rms (A)	THD (%)
A	15.69	118.13	30.1	102.91	22.03	110.02	27.04	73.43	33.95	73.83	37.3	64.72
B	14.13	118.08	30.11	102.99	19.88	109.99	24.39	81.15	33.26	72.15	36.09	62.27
C	16.92	146.46	34.14	119.17	20.82	119.86	26.83	87.87	38.1	94.38	39.98	83.30

Table 3
Summary of simulation results of the proposed control strategy with linear load under three cases.

Case	Source currents						Compensator currents		
	i_{sa}		i_{sb}		i_{sc}		i_{stab}	i_{stbc}	i_{stca}
	rms (A)	THD (%)	rms (A)	THD (%)	rms (A)	THD (%)	rms (A)	rms (A)	rms (A)
A	3.63	4.12	3.62	4.23	3.60	4.23	10.62	10.27	10.4
B	4.91	4.60	5.91	4.31	4.96	4.86	13.75	11.58	15.36
C	5.02	4.99	5.27	4.09	4.91	4.64	12.49	11.60	13.52

Table 4
Summary of simulation results of the proposed control strategy with non-linear unbalanced load under three cases.

Case	Source currents						Compensator currents		
	i_{sa}		i_{sb}		i_{sc}		i_{stab}	i_{stbc}	i_{stca}
	rms (A)	THD (%)	rms (A)	THD (%)	rms (A)	THD (%)	rms (A)	rms (A)	rms (A)
A	32.74	1.96	33.28	2.25	32.69	2.28	15.37	22.39	17.38
B	28.63	3.24	31.12	2.71	28.99	3.55	13.89	22.94	15.14
C	30.89	3.30	33.34	3.02	31.28	3.74	16.83	26.65	16.09

With reference to Tables 3 and 4, following observations are made for compensated system with delta connected linear/non-linear load under various source voltage conditions:

(i) Power factor correction is achieved for linear load. It results in reduction in reactive power supplied from source.
(ii) Unity source power factor is attained for non-linear load. Hence, source has to supply only average power to the load.
(iii) Balancing of source currents is achieved under all mentioned source voltage conditions.
(iv) The source VA is reduced due to reduction in rms value of source current after compensation.
(v) THD of compensated source current is within IEEE-519 standard harmonic current limits under various source voltage conditions.

5. Conclusion

In this paper, a scheme based on an improved instantaneous active and reactive current component theory is proposed for DSTATCOM installed in three-phase, three-wire system. The performance of the proposed scheme has been evaluated under balanced sinusoidal, unbalanced sinusoidal and unbalanced nonsinusoidal source voltage conditions in which delta connected linear as well as non-linear load situations are taken into account. The proposed scheme has been validated on a three-phase, three-wire distribution system using MATLAB/SIMULINK software. The simulation results showed that, if one seeks compliance with harmonics standards, imbalance elimination, power factor correction and source VA reduction, proposed scheme is capable of taking correct action under various source voltage and load conditions. In addition, the proposed scheme is capable to restrict THD of source current within IEEE-519 standard harmonic current limits under any condition of use.

Appendix A

System parameters	
Rated source voltage	230 V (rms value).
Supply frequency	50 Hz
Source parameters	R_s = 0.1 Ω, L_s = 0.01 mH
Compensator parameters	V_{dc} = 600 V, C_{dc} = 1000 μF, R = 0.5 Ω, L_f = 6 mH. The turn ratio of each transformer is assumed to be 1:1
Linear load	Case A: R_{lab} = 75 Ω, L_{lab} = 240 mH. Case B and Case C: R_{lab} = 75 Ω, L_{lab} = 240 mH, R_{lbc} = 35 Ω, L_{lbc} = 130 mH, R_{lca} = 50 Ω, L_{lca} = 190 mH
Non-linear load	Case A, B, C: L = 1 mH, C = 1000 μF, R_{lab} = 75 Ω, R_{lbc} = 35 Ω and R_{lca} = 50 Ω

References

[1] Acha E, Agelids V, Anaya-Lara O, Miller T. Power electronic control in electric systems. 1st ed. Newness power engineering series. Oxford; 2002.
[2] Akagi H, Watanabe EH, Aredes M. Instantaneous power theory and applications to power conditioning. New Jersey, USA: John Wiley & Sons; 2007.
[3] Fuchs Ewald F, Mausoum Mohammad AS. Power quality in power systems and electrical machines. London, UK: Elsevier Academic Press; 2008.
[4] Moreno-Munoz A. Power quality: mitigation technologies in a distributed environment. London: Springer-Verlag London limited; 2007.
[5] IEEE recommended practices and requirements for harmonics control in electric power systems. IEEE Std. 519; 1992.
[6] Ghosh A, Ledwich G. Power quality enhancement using custom power devices. Boston: Kluwer Academic Publishers; 2002.
[7] Chen B, Hsu Y. A minimal harmonic controller for a STATCOM. IEEE Trans Ind Electron 2008;55(2):655–64.

[8] Herrera RS, Salmeron P, Kim H. Instantaneous reactive power theory applied to active power filter compensation: different approaches, assessment, and experimental results. IEEE Trans Ind Electron Jan. 2008;55(1):184–96.
[9] Divan D, Bhattacharya S, Banarjee B. Synchronous frame harmonic isolator using active series filter. In: Proceedings of 4th European conference on power electronics and applications, Florence, Italy; 3–6 September, 1991. p. 3030–5.
[10] Ghosh A, Joshi A. The use of instantaneous symmetrical components for balancing a delta connected load and power factor correction. Electr Power Syst Res 2000;54:67–74.
[11] Singh B, Verma V. Selective compensation of power-quality problems through active power filter by current decomposition. IEEE Trans Power Deliv 2008;23(2):792–9.
[12] Lascu C, Asiminoaei L, Boldea I, Blaabjerg F. Frequency response analysis of current controllers for selective harmonic compensation in active power filters. IEEE Trans Ind Electron 2009;56(2):337–47.
[13] Luo A, Shuai Z, Zhu W, Shen ZJ. Combined system for harmonic suppression and reactive power compensation. IEEE Trans Ind Electron 2009;56(2):418–28.
[14] Shyu K-K, Yang M-J, Chen Y-M, Lin Y-F. Model reference adaptive control design for a shunt active-power-filter system. IEEE Trans Ind Electron 2008;55(1):97–106.
[15] Mohagheghi S, Valle Y, Venayagamoorthy GK, Harley RG. A proportional-integrator type adaptive critic design-based neurocontroller for a static compensator in a multimachine power system. IEEE Trans Ind Electron Feb. 2007;54(1):86–96.
[16] Shu Z, Guo Y, Lian J. Steady-state and dynamic study of active power filter with efficient FPGA-based control algorithm. IEEE Trans Ind Electron 2008;55(4):1527–36.
[17] Singh B, Solanki J. A comparison of control algorithms for DSTATCOM. IEEE Trans Ind Electron 2009;56(7).
[18] Soares V, Verdelho P, Marques G. An instantaneous active and reactive current component method for active filters. IEEE Trans Power Electron July 2000;15(4):660–9.
[19] Miller TJ. Reactive power control in electric systems. 1st ed. Willey-Interscience: New York; 1982.